RSC Advances

PAPER

View Article Online
View Journal | View Issue

Cite this: *RSC Adv.*, 2020, **10**, 37280

Three-dimensionally ordered macro–mesoporous CoMo bulk catalysts with superior performance in hydrodesulfurization of thiophene†

Guoliang Chen,[ab] Wenpeng Xie,[a] Qinghong Li,[a] Wentai Wang,[c] Liancheng Bing,[a] Fang Wang,[a] Guangjian Wang,[a] Chunyan Fan,[b] Shaomin Liu[b] and Dezhi Han*[a]

Received 20th August 2020
Accepted 5th October 2020

DOI: 10.1039/d0ra07153f

rsc.li/rsc-advances

The introduction of surfactants during the fabrication of hydrodesulfurization catalysts could not only tune the microstructure but also promote the dispersion of active components. In this work, CoMo bulk catalysts with the hierarchical structure of three-dimensionally ordered macro–mesopores were successfully fabricated by using a colloidal crystal template with the addition of PEG 400 and/or F127 surfactants. The obtained samples were characterized by various techniques, and the possible mechanism of the structure formation was also discussed. The characterization and evaluation results reveal that the addition of surfactants can promote the formation of the mesopores (3–4 nm) inside the macroporous walls of these bulk catalysts, which is essential for the increase of catalyst surface area, and the active sites for reaction. The CoMo–PF-1 catalyst displayed superior catalytic performance for thiophene hydrodesulfurization with the thiophene conversion of 99.4% under 1 MPa at 360 °C, which is much higher than that (77.8%) at 0.1 MPa. This result is even comparable to our previous report with the thiophene conversion of 99.2% over the 3DOM CoMo catalyst under 3 MPa.

1 Introduction

With the strict environmental regulations worldwide,[1] the hydrodesulfurization (HDS) process has attracted a lot of attention as an efficient technique to reduce sulfur content in transportation fuels. Currently, the supported Mo(W)S_2 with the assistance of the Co or Ni promoter is still the state of the art catalyst,[2–5] because of its high efficiency for the removal of sulfur-containing compounds and high stability in long-term operation. However, these supported catalysts hardly reduce the sulfur content to ultralow levels under mild conditions due to the limitation of active sites and unfavorable interaction between carrier and active metals. Besides, it is also difficult to acquire direct information about the inherent activity of active sites due to the interference of the support.[6]

Recently, the bulk catalysts consisted of two or more active components have been conceived as a viable alternative option for the updates of HDS catalysts.[6–11] Compared to the supported ones, the bulk catalysts without the support can generate a larger number of active sites after the pre-sulfurization treatment. Impressively, the NiMoW bulk catalyst showed the HDS activity three times higher than the traditional supported CoMo/γ-Al_2O_3 catalyst.[6] It is also possible to directly investigate the morphology and stacks of Mo(W)S_2 for further improving the HDS activity without the influence of support.[7,12,13] However, the absence of support would result in the poor dispersion of the active metals. Therefore, bulk catalysts usually exhibit much lower atom efficiency than some supported catalysts, which limits their application and development. To address the above issues, some researchers tried to increase the surface area of bulk catalysts by adding a wide variety of additives such as ethylene glycol, polyvinylpyrrolidone (PVP), and pluronic 123 (P123).[7,12–15] However, the utilization of active metals is still unsatisfactory. Therefore, it is still a challenging subject to search the highly efficient methods for the full utilization of active metals in bulk catalysts.

Nowadays, the hierarchical materials with three-dimensionally ordered macroporous (3DOM) structure fabricated by using the colloidal crystal template (CCT), such as PS,[16] PMMA[17] or SiO_2,[18] are widely used in many specific fields because of their novel physicochemical properties.[17,19–22] In our previous work,[23] the prepared 3DOM bulk catalysts with the micropore size (>150 nm) can not only supply more active centers but also reduce the mass transfer resistance of the reactants and products through the three-dimensionally porous network. Therefore, these 3DOM bulk catalysts exhibit superior

[a]State Key Laboratory Base of Eco-chemical Engineering, College of Chemical Engineering, Qingdao University of Science and Technology, Qingdao 266042, China. E-mail: handzh@qust.edu.cn

[b]WA School of Mines: Minerals, Energy and Chemical Engineering, Curtin University, GPO Box U1987, Perth, WA 6845, Australia

[c]Key Laboratory of Marine Chemistry Theory and Technology, Ministry of Education, College of Chemistry and Chemical Engineering, Ocean University of China, Qingdao 266100, China

† Electronic supplementary information (ESI) available. See DOI: 10.1039/d0ra07153f

HDS activity for thiophene conversion. However, one of the common drawbacks of 3DOM materials is the relatively low specific surface area,[24–27] which is also the main reason for the low atom efficiency of these materials. Thus, various surfactants were introduced into the catalyst precursor during the preparation process to increase the surface area.[28–32] Dai's group successfully fabricated the worm-hole-like mesoporous 3DOM MgO with surface area higher than 100 $m^2\ g^{-1}$.[32] In addition, the introduction of surfactants can also improve the dispersion of the active phase of the prepared catalysts, and further enhance the HDS performance.[12,13,33] Therefore, these results enlighten us to employ the surfactants to create the mesoporous pores in the walls of 3DOM bulk catalysts for improving their HDS activity.

In this work, the PEG400 and F127 surfactants were employed to develop 3DOM CoMo bulk catalysts with the mesoporous wall. The obtained CoMo bulk catalysts were characterized by various techniques and their HDS performance was tested in a fixed bed micro-reactor.

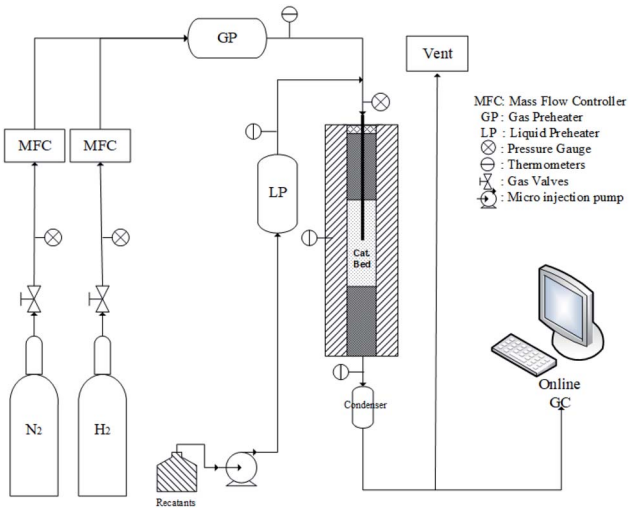

Fig. 1 The schematic diagram of the fixed-bed micro-reactor for catalyst activity test.

2 Experimental

2.1 Catalyst preparation

The preparation of the well-ordered polymethyl methacrylate (PMMA) hard template is similar to our previous work.[23,34] The three-dimensionally ordered macro–mesoporous CoMo bulk catalysts were synthesized by the CCT method.[34] Typically, 0.01 mol $Co(NO_3)_2 \cdot 6H_2O$ and $(NH_4)_6Mo_7O_{24}$ (molar ratio of Co/Mo = 2/1) was dissolved in 10.0 g of ethanol aqueous solution (50 wt%) under stirring at 35 °C for 2 h to obtain an orange-red transparent precursor solution. Then, 0.50 ml poly(ethylene glycol) (PEG400, molecular weight = 400) or/and F127 (0.50 g, 1.00 g or 2.00 g) with an average molecular weight of 12 600 g mol^{-1} were sequentially introduced into the above solution under stirring for another 1 h. Finally, the PMMA template (*ca.* 6.0 g) was soaked into the precursor solution for 4 h and filtered to remove the excess solution, followed by drying in a desiccator at room temperature for 12 h and in an oven at 40 °C for another 4 h. The calcination procedure consisted of two steps: (1) in nitrogen for 3 h at 300 °C, and (2) in air for 5 h at 400 °C with the heating rate of 1 °C min^{-1}.

The samples prepared with PEG 400 and F127 were referred as CoMo–PEG and CoMo–F127, respectively. The samples with the addition of PEG400 and F127 (molar ratio of PEG400/F127 = 35.2, 17.6, and 8.8) were denoted as CoMo–PF-1, CoMo–PF-2, and CoMo–PF-3, respectively. The 3DOM CoMo sample (denoted as CoMo) without the addition of the surfactants was also prepared for comparison purposes.

2.2 Catalysts characterization

The scanning electron microscopy (SEM, HITACHI S-4800) was used to investigate the morphologies of the CoMo bulk catalysts. The low-temperature N_2 adsorption–desorption experiments were performed on a Micromeritics Tristar II 3020 adsorption analyzer at −196 °C to determine the N_2 adsorption–desorption isotherms, surface areas of the samples. The crystalline phases of the samples were detected by the X-ray diffraction (XRD) tests on a Bruker AXS-D8 diffractometer with the Cu Kα radiation source in the range of 10°–70°. The thermogravimetric analysis (TGA) was carried out on a thermal analyser (Netzsch, STS 449F5 Jupiter) to study the thermal stability of these samples over 10–600 °C at the heating rate of 10 °C min^{-1}. The high-resolution transmission electron microscopy (HRTEM) was employed to further investigate the relationship between the MoS_2 active sites and thiophene conversion.

2.3 The evaluation of HDS performance

The HDS activity tests over the prepared CoMo bulk catalysts were carried out in a continuous high-pressure fixed-bed micro-reactor, as depicted in Fig. 1. A minor amount (0.8 g) of the bulk catalyst was loaded in the center of the reactor, and *in situ* pre-sulfurized by the mixture of 3.0 wt% CS_2 in cyclohexane at 210 °C for 2 h and subsequent 300 °C for 5.5 h under 3 MPa of H_2 pressure. The ramp rate in the *in situ* pre-sulfurization process was 3 °C min^{-1}. Then, the sulfurizing agent was altered to the solution of 0.5 wt% thiophene in octane under the WHSV of 7.8 h^{-1} and H_2/oil ratio of 500/1 (v/v), while the hydrogen pressure was reduced to 0.01 MPa. The ramp rate of 5 °C min^{-1} was applied in the following temperature for the HDS reaction. The product was analyzed by the gas chromatograph equipped with a flame detector. The catalyst activities were determined by the thiophene conversion. The steady-state conversion after 3 h reaction under the target temperature for each catalyst was used for the final performance comparison.

3 Results and discussion

Fig. 2 presents the SEM images of the prepared CoMo bulk catalysts. Except for CoMo–PF-3, the other samples possess the "inverse-opal" structure with three-dimensionally ordered macropores. The formation of the 3DOM structure can be

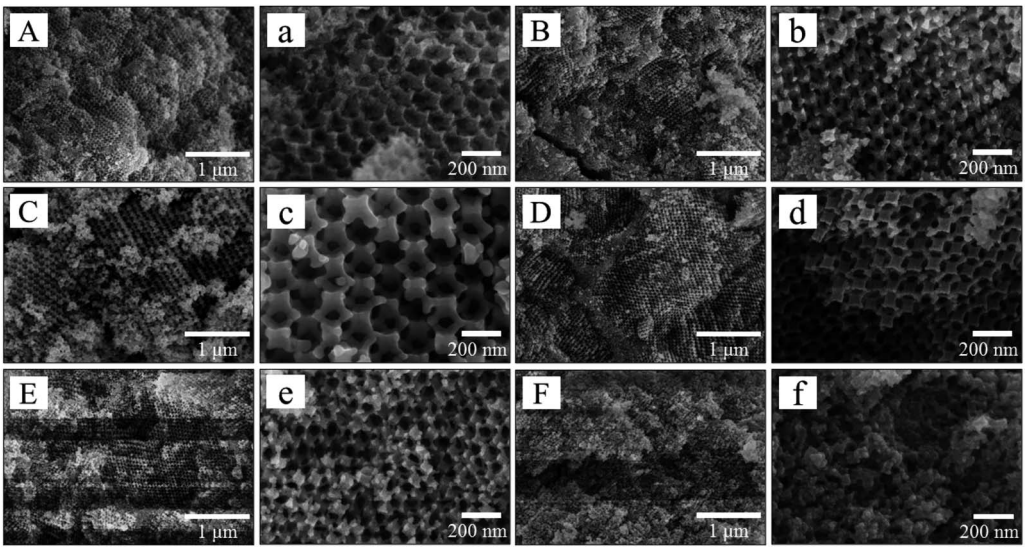

Fig. 2 The SEM images of the prepared CoMo bulk catalysts with three-dimensionally ordered macroporous structure ((A and a) CoMo; (B and b) CoMo–PEG; (C and c) CoMo–F127; (D and d) CoMo–PF-1; (E and e) CoMo–PF-2; (F and f) CoMo–PF-3).

controlled and tuned based on the well-ordered PMMA templates and other factors, such as the suitable precursor concentration, impregnation process, drying, and calcination conditions.[19,35] The macropore size of these CoMo bulk catalysts is around 150 nm, which is approximately equivalent to a 31% reduction compared to the initial microsphere particle size (220 nm) of PMMA due to the shrinkage of the template during the heat treatment procedure.[31,34] Besides, the introduction of a certain amount of PEG400 or F127 can benefit the formation of the high-quality 3DOM structure, while F127 with the high content (molar ratio of PEG400/F127 = 8.8) in the precursor can lead to the failure in the formation of 3DOM structure due to the high solution viscosity.[30,31] Furthermore, the TG and DTG curves (Fig. S1†) illustrate that the weight loss reaches a plateau when the temperature is higher than 400 °C, indicating the full elimination of the organic precursors in these catalysts. The 3DOM structure can supply more active sites for improving the HDS activity of the prepared CoMo bulk catalysts, as verified in the following discussion of the catalytic performance.

Moreover, the adsorption–desorption isotherms of all bulk CoMo samples can be classified to type-II with H3 hysteresis loop at the high relative pressure range (Fig. 3a), which is no adsorption platform with the elevated relative pressure. This indicates the pore size of the obtained bulk catalysts extends to

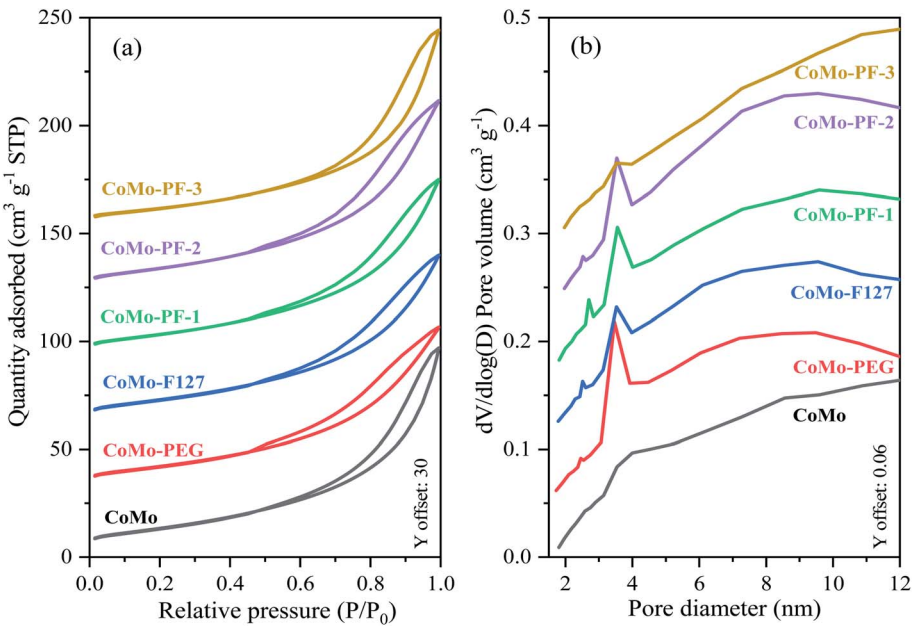

Fig. 3 The low-temperature N_2 adsorption–desorption curves (a) and the pore size distributions (b) of the obtained CoMo bulk catalysts.

Table 1 Preparation parameters and BET surface area of obtained CoMo bulk samples

Catalysts	Surfactant	(Co + Mo)/F127 (mol mol^{-1})	PEG 400/F127 (mol mol^{-1})	BET surface area (m^2 g^{-1})
CoMo	—	—	—	39.4
CoMo–PEG	PEG 400	—	—	44.9
CoMo–F127	F127	126/1	—	47.6
CoMo–PF-1	PEG400 + F127	63/1	35.2/1	48.4
CoMo–PF-2	PEG400 + F127	126/1	17.6/1	50.5
CoMo–PF-3	PEG400 + F127	252/1	8.8/1	42.5

the range of large pores,[24,25] which is consistent with the SEM characterization results from Fig. 2. Except for the CoMo and CoMo–PF-3, the pore size distributions of the other bulk catalysts in the Fig. 3b verify the existence of the mesopores (mostly 3–4 nm) in the macroporous wall, which reveals the positive effect of the surfactants on the formation of mesopores.[31,32] The existence of the mesoporous structure also can benefit the increase in the specific surface area of the prepared bulk catalysts, thus supply more active sites for HDS reaction. After the addition of the surfactants, the prepared bulk catalysts exhibited a much higher specific surface area compared to the CoMo catalyst prepared without the surfactant (Table 1). Especially, the specific surface area of the CoMo–PF-2 bulk catalyst is as high as 50.5 m^2 g^{-1}, which is equivalent to 28.2% enhancement as compared to that (39.4 m^2 g^{-1}) of the CoMo catalyst. However, it is difficult for the Co/Mo species to infiltrate into the interstices of the PMMA template due to the high-concentrated surfactants in the catalyst precursor, which can be responsible for the low specific surface area of the CoMo–PF-3 bulk catalyst.

Fig. 4a provides the XRD patterns of the CoMo bulk catalysts before sulfurization. All these samples exhibit the characteristic Co_3O_4 phase (JCPDS no. 43-2120) because of the relatively high loading of Co elements in these catalysts. The diffraction peaks at 26.5° and 23°correspond to β-$CoMoO_4$ (JCPDS no. 21-0868) with tetrahedral coordinated Mo atom.[36] Compared with the CoMo catalyst, the other catalysts exhibit the relatively high peak intensity of the β-$CoMoO_4$ crystalline phase, indicating that the surfactants PEG400/F127 are beneficial to the formation of the high-quality β-$CoMoO_4$ crystalline phase. The diffraction peaks at about 33° and 47° can be ascribed to the thermodynamically stable α-$CoMoO_4$ phase (JCPDS no. 25-1434) with octahedral coordinated Mo atom. After the sulfurization, it can be seen from the corresponding XRD patterns in Fig. 4b that all sulfurized catalyst exhibit the emergence of the Co_9S_8 phase (JCPDS no. 65-6801) with the disappearance of all oxide phases, indicating the high degree of sulfurization. Moreover, the MoS_2 with low-intensity characteristic diffraction peak (JCPDS no. 75-1539) is also observed in the sulfurized samples, implying that the weakly crystalline MoS_2 can be hardly detected by XRD.[37]

Fig. 5a shows the thiophene conversions over the prepared CoMo bulk catalysts in terms of temperature. All catalysts exhibit the progressively enhanced thiophene conversions with the increase in the reaction temperature, indicating that high temperature can lead to the acceleration of thiophene conversion due to the kinetically controlled process. The bulk catalysts prepared with the addition of surfactants, especially the CoMo–PF-1 catalyst, possess superior HDS performance in comparison with the CoMo catalyst. This could be attributed to the positive effects of the PEG400/F127 on the enhancement of specific surface area and the formation of abundant mesopores on the macropore walls of the prepared bulk catalysts. Moreover, the CoMo–PF-1 catalyst exhibits the relatively low stacks of MoS_2 for the maximum HDS activity due to the appropriate amount of F127 addition, which is in accordance with the results of the preparation of HDS catalysts with the addition of

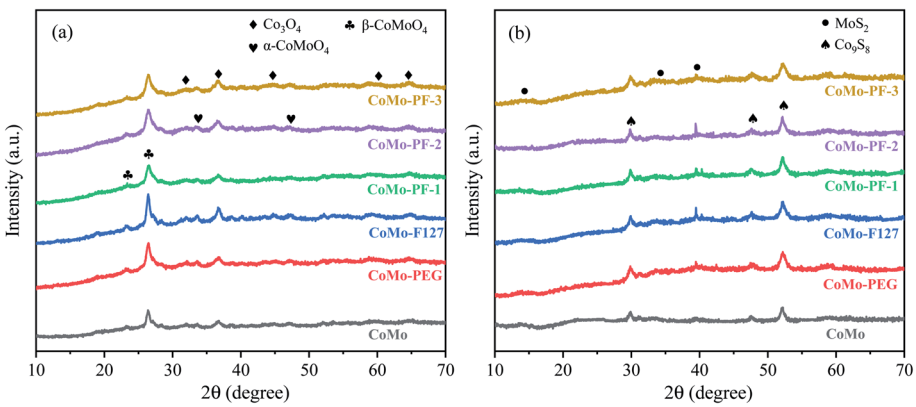

Fig. 4 The XRD patterns of CoMo bulk catalysts before (a) and after (b) sulfurization.

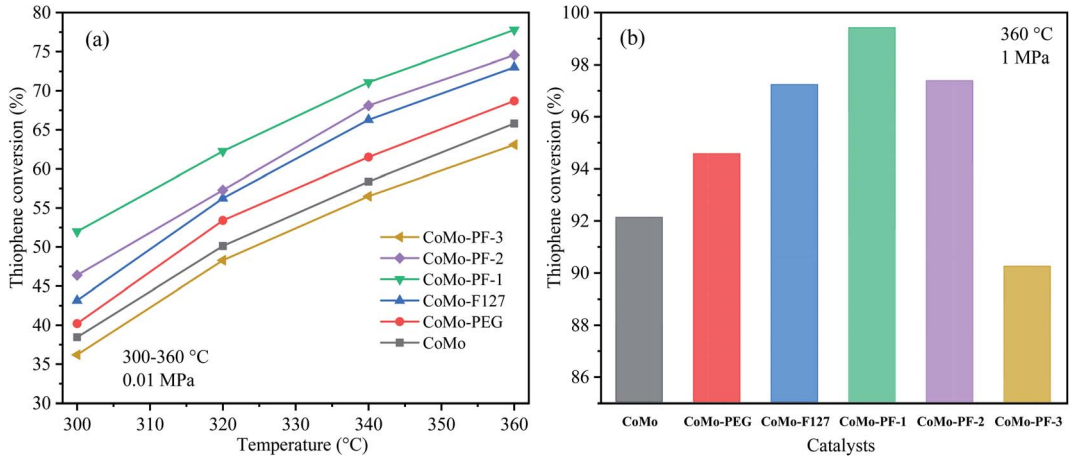

Fig. 5 The catalytic HDS activities of the CoMo bulk catalysts under different reaction conditions.

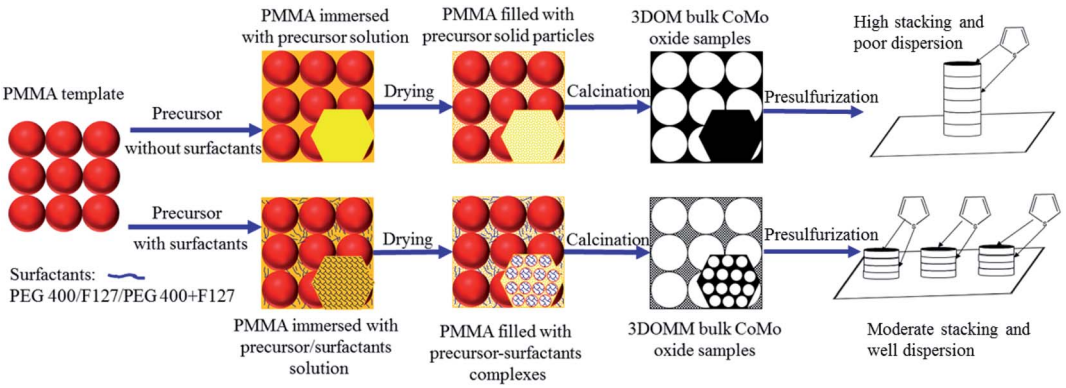

Fig. 6 The schematics of the fabrication of CoMo bulk catalysts with and without the surfactants.

surfactants.[12,13,38] And the failure in the formation of the 3DOM structure is responsible for the lowest thiophene conversion over the CoMo–PF-3 catalyst. After changing the reaction pressure from 0.1 to 1 MPa at 360 °C, the thiophene conversion over each bulk catalyst is significantly improved due to the enhancement of the contact between the H_2/thiophene and the active sites under the high pressure (Fig. 5b). The CoMo–PF-1 catalyst exhibited the maximum thiophene conversion of 99.4%, which is much higher than that (77.8%) at the reaction pressure of 0.1 MPa. This result is even comparable to our previous report with the thiophene conversion of 99.2% over the 3DOM CoMo catalyst under the H_2 pressure of 3 MPa.[23]

Generally, the HDS catalysts with the low stacking number of slabs and short slab length demonstrate the high dispersion of MoS_2, resulting in the high HDS activity as reported in previous literatures.[12,13,38,39] The HRTEM characterization results and the related calculation of MoS_2 dispersion were added in Fig. S2 and Table S1.† It can be observed that the addition of surfactants can significantly improve the dispersion of MoS_2 over the prepared bulk catalysts. Especially, the CoMo–PF-1 catalyst exhibits the shortest average length of 5.0 nm, the lowest stacking number of 3.3, and the high dispersion of MoS_2 of 0.24. This also can be the explanation of the HDS performance differences between the CoMo–PF-1 and CoMo–PF-2 catalysts, although the CoMo–PF-2 catalyst possesses the slightly higher surface area in comparison with the CoMo–PF-1 catalyst. Moreover, the thiophene conversions over the supported or bulk Mo-based HDS catalysts are listed in Table S2.† It can be seen that the CoMo–PF-1 catalyst exhibits a higher thiophene conversion than that of other catalysts available in the literatures under the relatively mild HDS conditions. The addition of surfactants in the bulk catalyst precursor can facilitate the formation of the mesopores in the macropore walls for enlarging the specific surface area of prepared bulk catalysts,[31,32] and also enhance the dispersion of the active MoS_2 phase,[12,13,38,39] as illustrated in Fig. 6.

4 Conclusions

The CoMo bulk catalysts with the hierarchical structure of three-dimensionally ordered macro–mesopores were successfully synthesized by using the colloidal crystal template with the addition of PEG400 or/and F127 surfactants. The presence of surfactants can promote the formation of the mesopores (3–4 nm) in the macroporous walls of the prepared bulk catalysts, which is essential to increase in the catalyst surface area and the active

sites for HDS reaction. Moreover, the high dispersion of MoS_2 over the bulk catalysts prepared with the assistance of these surfactants can be realized. The CoMo–PF-1 catalyst has the superior HDS catalytic performance with the thiophene conversion of 99.4% under 1 MPa at 360 °C in comparison with the other catalysts. This research would inspire us to develop the novel bulk catalysts with superior performance in the conversion of macromolecular reactants, such as protein and heavy oil.

Conflicts of interest

There are no conflicts to declare.

Acknowledgements

This work was supported by the Opening Fund of State Key Laboratory of Heavy Oil Processing (SKLOP202002002), National Natural Science Foundation of China (51602297), Natural Science Foundation of Shandong (ZR2019BB052, ZR2018027), Key Research and Development Project of Shandong Province (2019GGX103018), Fund of the State Key Laboratory of Chemical Resource Engineering, Beijing University of Chemical Technology (CRE-2018-C-3-2).

References

1 http://www.imo.org/en/MediaCentre/HotTopics/Pages/Sulphur-2020.aspx.
2 T. Huang, J. Xu and Y. Fan, Effects of concentration and microstructure of active phases on the selective hydrodesulfurization performance of sulfided $CoMo/Al_2O_3$ catalysts, *Appl. Catal., B*, 2018, **220**, 42–56.
3 M. Li, H. Li, F. Jiang, Y. Chu and H. Nie, The relation between morphology of $(Co)MoS_2$ phases and selective hydrodesulfurization for CoMo catalysts, *Catal. Today*, 2010, **149**, 35–39.
4 P. A. Nikulshin, V. A. Salnikov, A. V. Mozhaev, P. P. Minaev, V. M. Kogan and A. A. Pimerzin, Relationship between active phase morphology and catalytic properties of the carbon–alumina-supported Co(Ni)Mo catalysts in HDS and HYD reactions, *J. Catal.*, 2014, **309**, 386–396.
5 X.-l. Wang, Z. Zhao, Z.-t. Chen, J.-m. Li, A.-j. Duan, C.-m. Xu, D.-w. Gao, Z.-k. Cao, P. Zheng and J.-y. Fan, Effect of synthesis temperature on structure–activity-relationship over $NiMo/\gamma\text{-}Al_2O_3$ catalysts for the hydrodesulfurization of DBT and 4,6-DMDBT, *Fuel Process. Technol.*, 2017, **161**, 52–61.
6 S. Eijsbouts, S. W. Mayo and K. Fujita, Unsupported transition metal sulfide catalysts: from fundamentals to industrial application, *Appl. Catal., A*, 2007, **322**, 58–66.
7 P. Li, Y. Chen, C. Zhang, B. Huang, X. Liu, T. Liu, Z. Jiang and C. Li, Highly selective hydrodesulfurization of gasoline on unsupported Co–Mo sulfide catalysts: effect of MoS_2 morphology, *Appl. Catal., A*, 2017, **533**, 99–108.
8 Y. E. Licea, R. Grau-Crespo, L. A. Palacio and A. C. Faro, Unsupported trimetallic Ni(Co)–Mo–W sulphide catalysts prepared from mixed oxides: characterisation and catalytic tests for simultaneous tetralin HDA and dibenzothiophene HDS reactions, *Catal. Today*, 2017, **292**, 84–96.
9 A. N. Varakin, A. V. Mozhaev, A. A. Pimerzin and P. A. Nikulshin, Comparable investigation of unsupported MoS_2 hydrodesulfurization catalysts prepared by different techniques: advantages of support leaching method, *Appl. Catal., B*, 2018, **238**, 498–508.
10 L. Yue, G. Li, F. Zhang, L. Chen, X. Li and X. Huang, Size-dependent activity of unsupported Co–Mo sulfide catalysts for the hydrodesulfurization of dibenzothiophene, *Appl. Catal., A*, 2016, **512**, 85–92.
11 C. Zhang, P. Li, X. Liu, T. Liu, Z. Jiang and C. Li, Morphology–performance relation of $(Co)MoS_2$ catalysts in the hydrodesulfurization of FCC gasoline, *Appl. Catal., A*, 2018, **556**, 20–28.
12 V. Hetier, D. Pena, A. Carvalho, L. Courthéoux, V. Flaud, E. Girard, D. Uzio, S. Brunet, P. Lacroix-Desmazes and A. Pradel, Influence of Pluronic® P123 Addition in the Synthesis of Bulk Ni Promoted MoS_2 Catalyst. Application to the Selective Hydrodesulfurization of Sulfur Model Molecules Representative of FCC Gasoline, *Catalysts*, 2019, **9**, 793.
13 H. Liu, Q. Liu, J. Zhang, C. Yin, Y. Zhao, S. Yin, C. Liu and W. Sun, PVP-assisted synthesis of unsupported NiMo catalysts with enhanced hydrodesulfurization activity, *Fuel Process. Technol.*, 2017, **160**, 93–101.
14 H. Liu, C. Yin, X. Li, Y. Chai, Y. Li and C. Liu, Effect of NiMo phases on the hydrodesulfurization activities of dibenzothiophene, *Catal. Today*, 2017, **282**, 222–229.
15 A. Mansouri and N. Semagina, Promotion of Niobium Oxide Sulfidation by Copper and Its Effects on Hydrodesulfurization Catalysis, *ACS Catal.*, 2018, **8**, 7621–7632.
16 J. Wang, W. Zhang, Z. Zheng, Y. Gao, K. Ma, J. Ye and Y. Yang, Enhanced thermal decomposition properties of ammonium perchlorate through addition of 3DOM core–shell Fe_2O_3/Co_3O_4 composite, *J. Alloys Compd.*, 2017, **724**, 720–727.
17 J. Xiong, X. Mei, J. Liu, Y. Wei, Z. Zhao, Z. Xie and J. Li, Efficiently multifunctional catalysts of 3D ordered meso–macroporous $Ce_{0.3}Zr_{0.7}O_2$-supported $PdAu@CeO_2$ core–shell nanoparticles for soot oxidation: synergetic effect of $Pd–Au–CeO_2$ ternary components, *Appl. Catal., B*, 2019, **251**, 247–260.
18 H. Yang, J. Deng, S. Xie, Y. Jiang, H. Dai and C. T. Au, Au/MnO/3DOM SiO_2: highly active catalysts for toluene oxidation, *Appl. Catal., A*, 2015, **507**, 139–148.
19 H. Arandiyan, Y. Wang, H. Sun, M. Rezaei and H. Dai, Ordered meso- and macroporous perovskite oxide catalysts for emerging applications, *Chem. Commun.*, 2018, **54**, 6484–6502.
20 A. Vu, X. Li, J. Phillips, A. Han, W. H. Smyrl, P. Bühlmann and A. Stein, Three-Dimensionally Ordered Mesoporous (3DOM) Carbon Materials as Electrodes for Electrochemical Double-Layer Capacitors with Ionic Liquid Electrolytes, *Chem. Mater.*, 2013, **25**, 4137–4148.

21 Z. Wang, X. Fan, D. Han and F. Gu, Structural and electronic engineering of 3DOM WO_3 by alkali metal doping for improved NO_2 sensing performance, *Nanoscale*, 2016, **8**, 10622–10631.

22 S. Xie, H. Dai, J. Deng, Y. Liu, H. Yang, Y. Jiang, W. Tan, A. Ao and G. Guo, Au/3DOM Co_3O_4: highly active nanocatalysts for the oxidation of carbon monoxide and toluene, *Nanoscale*, 2013, **5**, 11207–11219.

23 G. Wang, G. Chen, W. Xie, W. Wang, L. Bing, Q. Zhang, H. Fu, F. Wang and D. Han, Three-dimensionally ordered macroporous bulk catalysts with enhanced catalytic performance for thiophene hydrodesulfurization, *Fuel Process. Technol.*, 2020, **199**, 106268.

24 X. Li, H. Dai, J. Deng, Y. Liu, Z. Zhao, Y. Wang, H. Yang and C. T. Au, In situ PMMA-templating preparation and excellent catalytic performance of Co_3O_4/3DOM $La_{0.6}Sr_{0.4}CoO_3$ for toluene combustion, *Appl. Catal., A*, 2013, **458**, 11–20.

25 X. Li, Y. Liu, J. Deng, S. Xie, X. Zhao, Y. Zhang, K. Zhang, H. Arandiyan, G. Guo and H. Dai, Enhanced catalytic performance for methane combustion of 3DOM $CoFe_2O_4$ by co-loading MnO and Pd–Pt alloy nanoparticles, *Appl. Surf. Sci.*, 2017, **403**, 590–600.

26 S. Xie, J. Deng, S. Zang, H. Yang, G. Guo, H. Arandiyan and H. Dai, Au-Pd/3DOM Co_3O_4: highly active and stable nanocatalysts for toluene oxidation, *J. Catal.*, 2015, **322**, 38–48.

27 K. Zhang, Y. Liu, J. Deng, S. Xie, H. Lin, X. Zhao, J. Yang, Z. Han and H. Dai, Fe_2O_3/3DOM $BiVO_4$: high-performance photocatalysts for the visible light-driven degradation of 4-nitrophenol, *Appl. Catal., B*, 2017, **202**, 569–579.

28 H. Arandiyan, H. Dai, J. Deng, Y. Liu, B. Bai, Y. Wang, X. Li, S. Xie and J. Li, Three-dimensionally ordered macroporous $La_{0.6}Sr_{0.4}MnO_3$ with high surface areas: active catalysts for the combustion of methane, *J. Catal.*, 2013, **307**, 327–339.

29 B. Liu, Y. Liu, C. Li, W. Hu, P. Jing, Q. Wang and J. Zhang, Three-dimensionally ordered macroporous Au/CeO_2–Co_3O_4 catalysts with nanoporous walls for enhanced catalytic oxidation of formaldehyde, *Appl. Catal., B*, 2012, **127**, 47–58.

30 Y. Liu, H. Dai, Y. Du, J. Deng, L. Zhang, Z. Zhao and C. T. Au, Controlled preparation and high catalytic performance of three-dimensionally ordered macroporous $LaMnO_3$ with nanovoid skeletons for the combustion of toluene, *J. Catal.*, 2012, **287**, 149–160.

31 R. Zhang, H. Dai, Y. Du, L. Zhang, J. Deng, Y. Xia, Z. Zhao, X. Meng and Y. Liu, P123–PMMA dual-templating generation and unique physicochemical properties of three-dimensionally ordered macroporous iron oxides with nanovoids in the crystalline walls, *Inorg. Chem.*, 2011, **50**, 2534–2544.

32 H. Li, L. Zhang, H. Dai and H. He, Facile synthesis and unique physicochemical properties of three-dimensionally ordered macroporous magnesium oxide, gamma-alumina, and ceria–zirconia solid solutions with crystalline mesoporous walls, *Inorg. Chem.*, 2009, **48**, 4421–4434.

33 L. van Haandel, G. M. Bremmer, E. J. M. Hensen and T. Weber, The effect of organic additives and phosphoric acid on sulfidation and activity of (Co)Mo/Al_2O_3 hydrodesulfurization catalysts, *J. Catal.*, 2017, **351**, 95–106.

34 D. Han, X. Li, L. Zhang, Y. Wang, Z. Yan and S. Liu, Hierarchically ordered meso/macroporous γ-alumina for enhanced hydrodesulfurization performance, *Microporous Mesoporous Mater.*, 2012, **158**, 1–6.

35 J. Fang, Y. Xuan and Q. Li, Preparation of three-dimensionally ordered macroporous perovskite materials, *Chin. Sci. Bull.*, 2011, **56**, 2156–2161.

36 A. L. B. Joaquin and L. Brito, Effect of phase composition of the oxidic precursor on the HDS activity of the sulfided molybdates of Fe(II), Co(II), and Ni(II), *J. Catal.*, 1997, **171**, 467–475.

37 C. Yin, Y. Wang, S. Xue, H. Liu, H. Li and C. Liu, Influence of sulfidation conditions on morphology and hydrotreating performance of unsupported Ni–Mo–W catalysts, *Fuel*, 2016, **175**, 13–19.

38 B. Yoosuk, C. Song, J. H. Kim, C. Ngamcharussrivichai and P. Prasassarakich, Effects of preparation conditions in hydrothermal synthesis of highly active unsupported NiMo sulfide catalysts for simultaneous hydrodesulfurization of dibenzothiophene and 4,6-dimethyldibenzothiophene, *Catal. Today*, 2010, **149**, 52–61.

39 A. Nogueira, R. Znaiguia, D. Uzio, P. Afanasiev and G. Berhault, Curved nanostructures of unsupported and Al_2O_3-supported MoS_2 catalysts: synthesis and HDS catalytic properties, *Appl. Catal., A*, 2012, **429–430**, 92–105.

